Group-Wise Registration of Point Sets for Statistical Shape Models

Abtin Rasoulian*, *Student Member, IEEE*, Robert Rohling, *Senior Member, IEEE*, and Purang Abolmaesumi, *Senior Member, IEEE*

***Abstract*—This paper presents a novel, fast, group-wise registration technique based on establishing soft correspondences between groups of point sets. The registration approach is used to create a statistical shape model, capable of learning the shape variations within a training set. The shape model consists of a mean shape and its transformations to all training shapes. We decouple the procedure into two steps: updating the mean shape and registering it to the training shapes. The algorithm alternates between these two steps until convergence. Following the generation of the statistical shape model, we use the soft correspondence approach to register the model to a new observation. We perform extensive experiments on two data sets: lumbar spine and hippocampi. We compare our algorithm to available state-of-the-art group-wise registration algorithms including feature-based and volume-based approaches. We demonstrate improved generalization, specificity and compactness compared to these algorithms.**

***Index Terms*—Gaussian mixture model, group-wise registration, statistical shape model.**

I. Introduction

STATISTICAL shape models (SSMs) are known to be a powerful tool in segmentation and shape analysis [15]. The *a priori* knowledge incorporated in these models greatly improves robustness of the segmentation to noise, artifacts, and missing data. A complete review on alternative approaches to SSMs are given by Heimann and Meinzer [22]. SSMs are usually built from a set of training shapes by learning the variations among them. This involves construction of a mean shape and its principal variations. Training shapes may be represented by point sets, curves, surfaces or volumes. Although a rich body of literature exists on the generation of shape models using volumetric data [3], [4], [8], [17], [24], [34], [38], [40], quite less is available over surfaces [14], [18], [20]. This is primarily due to the difficulty associated with establishing the correspondences between surfaces of the training shapes, which directly affects the model quality. Errors in establishing such correspondences can lead to large errors in shape variability and meaningless shape models.

The first attempt at generating SSMs [16] required manual landmark identification for establishing the point correspondence, generally a time consuming and subjective task. In order to automatically find exact one-to-one correspondences, others [10], [26] developed techniques to minimize the distances between corresponding points using variations of the iterative closest point (ICP) algorithm [7]. In these techniques, an arbitrary shape is chosen as the reference and registered to all other shapes in the training set. This technique is biased to the selection of the reference and may not represent all the possible variations [6]. Thus far, attempts to solve this problem by the supervised selection of the [11], [44] remain template-based and, hence, biased to the reference. To solve this problem, others developed group-wise registration [3], [8], [24], where both the mean shape and its transformation to the training shapes were considered unknown.

The two general approaches for performing a group-wise registration of shapes are the backward and the forward models. Durrlemann *et al.* [20] give a complete comparison between these two approaches. In the backward model, the mean shape is assumed to be a noisy observation of training shapes. Therefore, all shapes are deformed back to a common reference. The mean shape is then the by-product of this procedure and is reconstructed by averaging the deformed instances [14]. In the forward model, the training shapes are assumed to be the noisy observations of the deformed mean shape [20]. This assumption is less computationally intensive, and is always implemented by breaking the registration into two separate steps: 1) construction of the mean shape and 2) registration of the mean shape to training shapes. These steps are alternately performed in each iteration [24].

Surfaces are traditionally represented by point sets. However, such a representation is not suitable for group-wise registration. Discretization may prohibit exact one-to-one correspondences between two point sets; thus, the perfect matching of the underlying geometries is not guaranteed. To address this problem, many used other representations of surfaces such as triangulated surfaces [20], parametric representation [18], medial axes [31], and probabilistic distributions [12], [39]. Such representations, however, lead to large computational complexity in the registration step.

To improve the run-time, Chui and Rangarajan developed an algorithm that took point sets as input [14]. They extended

Manuscript received March 28, 2012; revised May 22, 2012; accepted May 26, 2012; first published June 5, 2012. Date of publication June 05, 2012; date of current version October 26, 2012. This work was supported by grants from the Natural Sciences and Engineering Research Council of Canada (NSERC) and the Canadian Institutes of Health Research (CIHR). *Asterisk indicates corresponding author.*

*A. Rasoulian is with the Department of Electrical and Computer Engineering, University of British Columbia, Vancouver, BC, V6T 1Z4 Canada (e-mail: abtinr@ece.ubc.ca).

P. Abolmaesumi are with the Department of Electrical and Computer Engineering, University of British Columbia, Vancouver, BC, V6T 1Z4 Canada (e-mail: purang@ece.ubc.ca).

R. Rohling is with the Department of Electrical and Computer Engineering and Department of Mechanical Engineering, University of British Columbia, Vancouver, BC, V6T 1Z4 Canada (e-mail: rohling@ece.ubc.ca).

Color versions of one or more of the figures in this paper are available online at http://ieeexplore.ieee.org.

Digital Object Identifier 10.1109/TMI.2012.2202913

soft correspondences, a technique originally developed to register two point sets using a deformable transformation [13]. Unlike ICP, this technique establishes probabilistic and not exact one-to-one correspondences between point sets. Specifically, they use the backward model to produce an unbiased mean shape. The backward model, however, is computationally intensive [20]. To address this problem, Hufnagel *et al.* [23] developed a forward modelling technique to build SSMs. Unlike Chui and Rangarajan, they utilized an affine transformation to register the mean shape to the training shapes. The affine transformation may lead to a large residual between the registered mean shape and the training shapes. Consequently, the model is not accurate and not capable of generating all possible variations.

The following contributions are made.

- First, we introduce a novel technique for group-wise registration of a group of point sets, referred to as group-wise Gaussian mixture model (GMM)-based registration. We use the forward modeling and deformable registration to generate the mean shape and its variations. We decouple the group-wise registration into two steps: registration using a nonrigid transformation and updating the mean shape. The registration is performed using an expectation-maximization algorithm [30] and the mean shape is updated using the Quasi-Newton method. The nonrigid transformation is considered as a probability density estimation problem. The points in the mean shape (moving point set) are assumed to be centeroids of a GMM and the points in the training sets (fixed point set) are the observations. The points in moving set are forced to move locally coherent to preserve the topological structure and additionally maximize the likelihood of the GMM generating the observations.
  We perform extensive experiments on two data sets: L2 vertebrae and hippocampi. We compare our algorithm to available state-of-the-art group-wise registration algorithms including feature-based and intensity-based approaches. Specifically, we use the following approaches.
  - Intensity-based method proposed by Balci *et al.* [4] that is publicly available.
  - Feature-based method proposed by Styner *et al.* [36] that is publicly available.
  - Our implementation of a feature-based method proposed by Hufnagel *et al.* [23].
  - Our implementation of a feature-based method proposed by Chui and Rangarajan [14].
- Second, we utilize the probabilistic approach to register the SSM to each new instance. Our algorithm performs a global search to find the parameters for instantiating the SSM. We perform experiments on lumbar vertebrae to investigate the behavior of our algorithm to the presence of noise and outliers.

The rest of this paper is organized as follows. In Section II, we provide an overview of the group-wise GMM-based registration technique. Then, we explain the SSM reconstruction using the result of the group-wise registration. Next, we illustrate our technique for registration of the SSM to a new instance. In Section III, the evaluation method of the proposed techniques is presented and results are given in Section IV. Sections V and VI discuss and conclude the paper.

II. Methods and Materials

A. Methods

The methods are presented in this section as follows. Section II-A1 introduces the GMM-based group-wise registration algorithm. Section II-A2 describes the reconstruction of the SSM using the result of the group-wise registration.Section II-A3 presents the algorithm for registration of an SSM to a new subject.

1) Group-Wise GMM-Based Registration Algorithm: The objective of the group-wise registration process is to extract statistical properties of a particular shape within a training population. In the context of statistical shape models, this procedure normally results in a mean shape and its variations. The variations are usually derived by registration of the mean shape to all training shapes.

The surface points can be considered as observations of a probability distribution. Having this assumption, the registration of two point sets is converted to a probability density estimation problem, where one point set represents a distribution, and the other one represents the data points. Good candidates for representing such distributions are mixture models. The GMM [27], which is widely used in pattern recognition and machine learning [9], has been utilized as the model in our work. The mixture is defined by a convex combination of *Gaussian components*, each presented by a mean point and a variance.

Following the probabilistic registration scheme, points in the mean shape are assumed to be the centroids of a GMM that generates the training shape.

Throughout the paper, the following notation is used.

K	Number of training data sets.
D	Dimension of the point sets, i.e., 2-D or 3-D.
N_k	Size of the kth training point set.
$\mathbf{T}_{k(N_k \times D)}$	kth training point set.
$\mathbf{t}_n^k$	nth point of the kth training point set.
M	Number of points in the mean shape.
$\mathbf{Z}_{M \times D}$	Mean shape.
$\mathbf{z}_m$	mth point of the mean shape.
σ	Variance of the Gaussian components.
Φ_k	Transformation from the mean shape to kth training point set.

For simplicity, we assume the same isotropic variance in all directions, $\sigma\mathbf{I}$, for all Gaussian components.

Based on the forward model, training shapes, $\mathbf{T}_k$, are noisy observations of the deformed mean shape, $\mathbf{Z}$, by the transformation Φ_k

$$\mathbf{T}_k = \Phi_k(\mathbf{Z}) + \epsilon_k. \tag{1}$$

The unknowns are $\mathbf{Z}$ and Φ_k, while ϵ_k is an independent and identically distributed Gaussian noise component. The problem

is defined as a maximum a posteriori (MAP) estimation for independent observations and can be solved by minimizing the log-likelihood function

$$E(\Phi_k, \mathbf{Z}) = -\sum_{k=1}^{K}\sum_{n=1}^{N_k}\log\sum_{m=1}^{M} P(\mathbf{z}_m)P(\mathbf{t}_n^k|\Phi_k(\mathbf{z}_m)) \quad (2)$$

where Φ_k is a displacement function and is defined discretely over points in $\mathbf{Z}$. The unknowns, $\mathbf{Z}$ and Φ_k, are found using an expectation-maximization (EM) algorithm [27]. The expectation part computes the probability of how likely a point in the mean shape generates another point in a training point set

$$P(\mathbf{z}_m|\mathbf{t}_n^k) = \frac{\exp\left(-\frac{1}{2}\left\|\frac{\mathbf{t}_n^k - \Phi_k(\mathbf{z}_m)}{\sigma}\right\|^2\right)}{\sum_{j=1}^{N_k}\exp\left(-\frac{1}{2}\left\|\frac{\mathbf{t}_j^k - \Phi_k(\mathbf{z}_m)}{\sigma}\right\|^2\right)}. \quad (3)$$

Initially, σ, the variance of the Gaussian components, is chosen to be large. Its value decreases in each iteration. Parameters are updated in the maximization step. The following objective function is minimized:

$$(\mathbf{Z}^*, \Phi_k^*) = \arg\min_{\mathbf{Z},\Phi_k}\sum_{k=1}^{K} Q(\mathbf{Z}, \Phi_k) \quad (4)$$

where

$$Q(\mathbf{Z}, \Phi_k) = \frac{1}{2\sigma^2}\sum_{m,n=1}^{M,N_k} P(\mathbf{z}_m|\mathbf{t}_n^k)\|\mathbf{t}_n^k - \Phi_k(\mathbf{z}_m)\|^2 + \frac{\gamma}{2}\|\mathbf{L}\Phi_k\|^2. \quad (5)$$

The latter term, $\|\mathbf{L}\Phi_k\|$, is a regularization over the transformations and is controlled by a "trade-off" variable γ. The objective function can be minimized alternately with respect to the mean shape and the transformation parameters. For a fixed mean shape, the problem becomes a pair-wise registration problem and each term of (5) can be minimized separately. The pair-wise registration for a given $\mathbf{T}_k$ and $\mathbf{Z}$ is stated and solved by Myronenko *et al.* [30]. They modeled the transformation to be a displacement field defined over each point belonging to the mean shape. They also defined the regularization over transformation function by

$$\|\mathbf{L}\Phi_k\|^2 = \int_{R^D}\frac{|\tilde{\Phi}_k(s)|^2}{\tilde{G}(s)}ds. \quad (6)$$

The function $\tilde{\Phi}_k$ indicates the Fourier transform of the function Φ_k. $\tilde{G}$ represents a symmetric positive-definite low pass filter. The integral thus measures the energy at high frequencies. In the implementation, $\tilde{G}$ is represented by a Gaussian kernel with standard deviation β, set initially by the user. This variable controls the locality of the coherency between point transformations. A higher value of β results in more regularized transformations. For a detailed discussion on the difference between β and γ, we invite the reader to refer to [41].

Myronenko *et al.* used the idea of coherent point drift [42] to model the deformations and solved the M-step in a closed-form solution [30]. For fixed transformations, each point of the mean shape, $\mathbf{z}_m$, can be found separately by minimizing

$$\mathbf{Z}^* = \arg\min_{\mathbf{Z}}\sum_{k=1}^{K}\sum_{n=1}^{N_k} P(\mathbf{z}|\mathbf{t}_n^k)\|\mathbf{t}_n^k - \Phi_k(\mathbf{z}_m)\|^2. \quad (7)$$

The transformations, Φ_k, are discrete functions defined over initial position of the mean shape points, $\mathbf{z}_m$. To find $\Phi_k(p)$ for an arbitrary point, $\mathbf{p}$, interpolation should be performed. To reduce the amount of computation, the transformation is coded in grid points. A thin-plate spline interpolation using grid points is used. The new $\mathbf{z}_m$ is found by minimizing the cost function defined in (7). The Broyden–Fletcher–Goldfarb–Shanno (BFGS) Quasi-Newton method, with a cubic line search, is used as the optimizer.

We initialize the group-wise GMM-based registration algorithm by setting the mean shape to an arbitrary shape. We found that the result of the algorithm is not sensitive to the mean shape initialization. The transformations from the mean shape to the training shapes are set to identity. The atlas estimation algorithm is written as follows.

Require: Group of point sets $\mathbf{T}_k$

Initialize $\mathbf{Z}$ and Φ_k

Bring all point sets to the same coordinate system by rigidly registering all to one selected randomly from the training set.

repeat

for all $\mathbf{T}_k$ **do**

Update Φ_k by registering $\mathbf{Z}$ to $\mathbf{T}_k$

end for

Update mean shape $\mathbf{Z}$ by minimizing Equation **(7)**

until converge

In the actual implementation, it is more efficient to only update the mean shape after several iterations of the registration. In particular, each iteration of the registration includes updating the probability function, $P(\mathbf{z}|\mathbf{t}_n^k)$, and computing the transformations, Φ_k, that minimize the cost function in (5). Additionally, performing the group-wise registration using affine transformations (as was generated by Hunfangel *et al.* [23]) and passing the results as an initialization to the nonrigid transformation step, improves the computation speed substantially. The algorithm convergence criterion is the value of σ being less than a threshold, θ. A suitable value for such threshold can be calculated from the data, such as the average distance between points, and is set at 0.01 mm for all tests. In summary, the behavior of the group-wise GMM-based registration algorithm is mainly determined by γ, the "trade-off" variable, and β, the regularization factor. Higher values for these variables result in smoother transformations.

2) Statistical Shape Model: The model can be built from the mean shape, $\mathbf{Z}$, and its transformations, Φ_k, to each subject. Any bias in the transformation, including translations

and rotations, are removed using Procrustes analysis [19]. Each transformation can be described by a $3M$ vector as: $\mathbf{V}_k = [\Phi_k(\mathbf{z}_1)^{\mathrm{T}} \dots \Phi_k(\mathbf{z}_M)^{\mathrm{T}}]^{\mathrm{T}}$. The average transformation is $\bar{\mathbf{V}} = 1/K \sum_{k=1}^{K} \mathbf{V}_k$. The covariance matrix is given by

$$S = \frac{1}{K-1} \sum_{k=1}^{K} (\mathbf{V}_k - \bar{\mathbf{V}})(\mathbf{V}_k - \bar{\mathbf{V}})^{\mathrm{T}}. \tag{8}$$

An eigen-decomposition on S delivers the principal modes of variation $\mathbf{\Psi}_k$ (eigenvectors) and their respective variances λ_k (eigenvalues). Eigenvectors are ordered with respect to their corresponding eigenvalues. By using only c modes, the SSM can be instantiated as follows:

$$\tilde{\mathbf{Z}} = \mathbf{Z} + \sum_{k=1}^{c} \mathbf{\Psi}_k b_k \tag{9}$$

for arbitrary selection of b_k.

3) Registering the Model to a New Subject: Available techniques for instantiation and registration of an SSM to a new instance, usually referred to as active shape model (ASM) search algorithms, commonly rely on performing a search along the normal to the SSM surface to find the edges and instantiating the SSM to minimize the distance of the SSM to these edges. However, this approach is known to be sensitive to noise and outliers [1]. Many modifications are applied to the original ASM implementation. Some address better selection of the landmarks in the image [28], [35], and others improve the shape parameters estimation [1], [25].

Rogers and Graham [32] investigate different approaches to robustly estimate the shape parameters. In particular they compare the M-estimators and random sampling approaches. M-estimators mainly rely on weighting strategies to reduce the effect of outliers and noisy observations. Lower weights are given to landmarks with higher residuals. Random sampling strategies on the other hand, try to find a small subset of landmarks, which contain only good data. RANSAC [21] and LMedS [33] are used as random sampling algorithms and both show superior performance over M-estimators in the presence of outliers. Other weighting strategies have also been proposed by Li and Chutatape [25].

Available techniques for instantiation and registration of an SSM to a new instance, usually referred to as ASM search algorithms, commonly rely on performing a search along the normal to the SSM surface to find the edges and instantiating the SSM to minimize the distance of the SSM to these edges. This is however shown to be not robust [1]. We propose a GMM-based approach (referred to as GMM-ASM hereafter) to register the model ($\mathbf{Z}$ with points $\mathbf{z}_m,\ m = 1 \dots M$) to a new instance ($\mathbf{T}$ with points $\mathbf{t}_n,\ n = 1 \dots N$). The new instance is the observation generated by a GMM, which is defined by the SSM mean shape points as its centroids. The SSM mean shape (here the moving set) can be instantiated using (9). We use the EM algorithm to find the parameters for instantiation of the SSM. The Expectation part of the algorithm is the same and appeared in (3). The same as before, σ, the variance of the Gaussian components, is initially chosen to be large. Its value decreases in each iteration. In the Maximization step, the following objective function is minimized:

$$Q(\mathbf{b}) = \sum_{m,n=1}^{M,N} P(\mathbf{z}_m|\mathbf{t}_n) \|\mathbf{t}_n - (\mathbf{z}_m + \boldsymbol{\psi}_m \mathbf{b})\|^2 + \mu \mathbf{b}^{\mathrm{T}} \mathbf{\Lambda} \mathbf{b} \tag{10}$$

and

$$\mathbf{b}^* = \arg\min_{\mathbf{b}} Q \tag{11}$$

where vector $\mathbf{b}_{c\times 1}$ holds the shape parameters. The latter term in (10) is the Tikhonov regularization over the shape parameters and is controlled by the trade-off variable μ. Matrix $\mathbf{\Lambda}$ is diagonal with elements $1/\lambda_k$. Matrix $\psi_{m3\times c}$ is made by concatenation of the parts of the vectors Ψ_m that correspond to the point $\mathbf{z}_m$ as

$$\boldsymbol{\psi}_m = [\mathbf{\Psi}^{\mathrm{T}}_{1\{3m\dots 3m+2\}} \dots \mathbf{\Psi}^{\mathrm{T}}_{c\{3m\dots 3m+2\}}]^{\mathrm{T}}. \tag{12}$$

In order to find the optimum weights, $\mathbf{b}$, we expand (10) as

$$\begin{aligned} Q = \sum_{m,n=1}^{M,N} P(\mathbf{z}_m|\mathbf{t}_n)(\mathbf{t}_n^{\mathrm{T}}\mathbf{t} + \mathbf{z}_m^{\mathrm{T}}\mathbf{z}_m + \mathbf{b}^{\mathrm{T}}\boldsymbol{\psi}_m^{\mathrm{T}}\boldsymbol{\psi}_m\mathbf{b} \\ -2\mathbf{z}_m^{\mathrm{T}}\mathbf{t}_n - 2\mathbf{z}_m^{\mathrm{T}}\boldsymbol{\psi}_m\mathbf{b} + 2\mathbf{t}_n^{\mathrm{T}}\boldsymbol{\psi}_m\mathbf{b}) + \mu\mathbf{b}^{\mathrm{T}}\mathbf{\Lambda}\mathbf{b}. \end{aligned} \tag{13}$$

By differentiation we have

$$\begin{aligned} \frac{\partial Q}{\partial b} = -2 \sum_{m,n=1}^{M,N} P(\mathbf{z}_m|\mathbf{t}_n)(\boldsymbol{\psi}_m^{\mathrm{T}}\boldsymbol{\psi}_m\mathbf{b} - \mathbf{z}_m^{\mathrm{T}}\boldsymbol{\psi}_m + \mathbf{t}_n^{\mathrm{T}}\boldsymbol{\psi}_m) \\ +\mu\mathbf{\Lambda}\mathbf{b}. \end{aligned} \tag{14}$$

If

$$\begin{aligned} \mathbf{\Upsilon} &= \sum_{m,n=1}^{M,N} P(\mathbf{z}_m|\mathbf{t}_n)\boldsymbol{\psi}_m^{\mathrm{T}}\boldsymbol{\psi}_m + \mu\mathbf{\Lambda}, \\ \mathbf{\Gamma} &= \sum_{m,n=1}^{M,N} P(\mathbf{z}_m|\mathbf{t}_n)(\mathbf{t}_n^{\mathrm{T}}\boldsymbol{\psi}_m - \mathbf{z}_m^{\mathrm{T}}\boldsymbol{\psi}_m) \end{aligned} \tag{15}$$

the optimum parametrization can be achieved by

$$\mathbf{b}^* = \Gamma\Upsilon^{-1}. \tag{16}$$

The algorithm steps are outlined below.

Require: $\mathbf{Z}$, $\mathbf{\Psi}$, λ, and $\mathbf{T}$

Initialize $\tilde{\mathbf{Z}} = \mathbf{Z}$ and σ

Construct $\boldsymbol{\psi}_m$

repeat

Construct $P(\mathbf{z}_m|\mathbf{t}_n)$ from $\tilde{\mathbf{Z}}$ and $\mathbf{T}$

Find $\mathbf{\Gamma}$ and $\mathbf{\Upsilon}$ using **(15)**

$\mathbf{b} = \mathbf{\Gamma}\mathbf{\Upsilon}^{-1}$

Decrease σ and $\tilde{\mathbf{Z}} = \mathbf{Z} + \Phi\mathbf{b}$

until converge

B. Materials

1) Data: Quantitative experiments were carried out on two different data sets: human L2 lumbar vertebra and hippocampus.

Vertebrae were manually segmented from a set of CT images captured from 45 patients undergoing CT imaging at Kingston General Hospital, Kingston, ON, Canada ($n = 36$) and at Vancouver General Hospital, Vancouver, BC, Canada ($n = 9$). Written informed consent was obtained from all patients. The manual segmentation was performed using ITK-SNAP [42]. The CT imaging resolution ranged from $0.6\,\mathrm{mm} \times 0.6\,\mathrm{mm} \times 0.6\,\mathrm{mm}$ to $0.97\,\mathrm{mm} \times 0.97\,\mathrm{mm} \times 3.2\,\mathrm{mm}$ spacing. 45 L2 vertebrae were used as the training set. The vertebrae had sizes between $47\,\mathrm{mm} \times 64\,\mathrm{mm} \times 47\,\mathrm{mm}$ and $87\,\mathrm{mm} \times 95\,\mathrm{mm} \times 61\,\mathrm{mm}$. The second dataset we used was the publicly available 42 segmented hippocampi from Styner *et al.* [36]. The hippocampi had sizes between $20\,\mathrm{mm} \times 35\,\mathrm{mm} \times 17\,\mathrm{mm}$ and $26\,\mathrm{mm} \times 41\,\mathrm{mm} \times 24\,\mathrm{mm}$.

2) Objective Metrics for Evaluating Statistical Shape Models: Evaluations are based on the distances between an instantiated SSM and the target surface. To compute the surface distances, both the instantiated SSM and the test data are triangulated using the Crust algorithm [2]. The distances from vertices of the two surfaces are computed. The rms of these distances is the first measure we have used and hereafter is referred to as rms distance. The maximum of these distances is the second measure and is called the Hausdorff distance. The proposed group-wise registration algorithm, i.e., the group-wise GMM, is evaluated by computing well-known measures of generalization, specificity, and compactness [37]. All measures are provided as a function of, c, the number of modes used in SSM instantiation.

An SSM with high generalization capability can adopt to a new observation that comes from the same anatomy. Generalization can be measured using the leave-one-out method: A model is built using all but one member of the training set and then fitted to the excluded member. The accuracy to which the model can describe the unseen member is measured using

$$G(c) = \frac{1}{K}\sum_{i=1}^{K} \mathbb{D}(\bar{S}_i, S_i) \tag{17}$$

where $\mathbb{D}(\bar{S}_i, S_i)$ can be the rms or Haussdorf distance between two surfaces. S_i is the left out member and $\bar{S}_i$ is the instantiated and registered SSM.

The specificity measures the ability to represent only valid instances of the object. To calculate it, the SSM is randomly instantiated within the range of valid parameters, $[-3\lambda \quad +3\lambda]$, and is rigidly registered to all members of the training set

$$S(c) = \frac{1}{R}\sum_{n=1}^{N} \mathbb{D}(\bar{S}_n, S_n) \tag{18}$$

where R is the number of the trials and S_n is the member of the training set with lowest rms distance error to the instantiated shape model $\bar{S}_n$.

The compactness is the ability to use a minimal set of parameters. This can be measured using the cumulative variance for the first c modes of the model

$$C(c) = \frac{\sum_{i=1}^{c} \lambda_i}{\sum_{i=1}^{K-1} \lambda_i}. \tag{19}$$

III. Experiments

A. Group-Wise GMM-Based Registration Algorithm Parameters

The behavior of the group-wise GMM-based registration algorithm is governed by two parameters, λ and β. The experiments were performed for various combinations of γ and β, where γ ranges between $[2^{-3} \quad 2^{-2} \ldots 2^{6}]$ and β ranges between $[2^{-3} \quad 2^{-2} \ldots 2^{3}]$. This covers a wide region around the proposed values by Myronenko *et al.* [29] $(\gamma, \beta = 1.0)$.

The generalization was reported for each combination of these two variables. The compactness was also computed as number of modes that cover 95% of the variations

$$\text{minimum} \quad r \quad \text{such that} \quad \frac{\sum_{i=1}^{r} \lambda_i}{\sum_{i=1}^{N} \lambda_i} > 0.95. \tag{20}$$

B. Comparison to Other Methods

For each data set, i.e., L2 vertebrae and hippocampi, the shape models were built using the group-wise GMM-based registration algorithm and compared to other available state-of-the-art methods. The first compared method is based on affine registered point sets using EM-ICP as proposed by Hufnagel *et al.* [23]. This is the most similar algorithm to the one proposed here with the key difference in the type of transformation. We also compared our method to the one proposed by Chui and Rangarajan [14]. This is also very similar to our method except that they follow a backward method to reconstruct the mean shape. The same experiments were also performed on SPHARM-PDM, a method proposed by Styner *et al.* [36]. In their approach, the corresponding points in the training shape surfaces are found by converting the surfaces into a spherical harmonic description.

The proposed algorithm was also compared to an intensity-based group-wise registration algorithm proposed by Balci *et al.* [4] that is referred to as " *congealing*" hereafter. In this work, deformations are modeled by B-splines and the objective function is entropy-based and defined in a group-wise framework. The open source implementation of the registration algorithm is available in ITK [5].

C. GMM-ASM Algorithm

We evaluated the robustness of the GMM-ASM algorithm proposed for registration of the SSM to a new subject and compared it to the original ASM search approach [16].

Two sets of experiments were performed. In the first experiment, an SSM of the L2 vertebra was reconstructed using the proposed group-wise GMM-based algorithm. A target was generated by randomly instantiating the SSM by giving random weights to the SSM modes and transforming using translation and rotation parameters drawn randomly within ± 5 mm and ± 5 mm degrees, using a uniform distribution. Then outliers were added to the target. The outliers were points randomly generated with a uniform distribution around the target. The SSM was registered to the target using four different algorithms, the original ASM, weighted least squares ASM

(WLS-ASM), LMedS-ASM, and GMM-ASM. In the original ASM implementation, the parameters are estimated to minimize the sum of squares of residuals between the shape and the data. In the WLS-ASM approach, the residual is minimized using a weighted least squares technique, where the weighting strategy proposed by Huber [45] is utilized. LMedS-ASM is also implemented using the approach presented by Rogers and Graham [46]. LMedS is a random sampling approach to fit a model into noisy data by minimizing the median of the residual. The fitting procedure was repeated 100 times for different percentages of outliers $[0\% - 40\%]$.

In the second experiment, we followed the same steps taken in the first experiments, except that the instance points were perturbed by a zero mean additive noise with known standard deviation.

The average distance between the corresponding points in the target and the registered SSM was reported as the target registration error (TRE). Registrations with a TRE below 3 mm were considered as successful.

IV. Results

A. Group-Wise GMM-Based Registration Algorithm Parameters

Fig. 1(a) and (c) show the average rms distance error for SSM built from group-wise GMM-based registration algorithm applied to both datasets using different values of γ and β. Higher values of these parameters constrain the deformation of the mean shape in the registration step and consequently produce a larger error. Thus, the model may not cover all the variations. On the other hand, the resulted model is more compact. Lower values of these variables remove all regularization over deformation of the mean shape and consequently, the variation modes are more noisy. Thus, the SSM is not capable of properly reconstructing an unseen observation. The selection of these two variables is a trade-off between compactness of the model and its generalization ability. Fig. 1(b) and (d) show the compactness of the resulted SSMs using different values of these parameters.

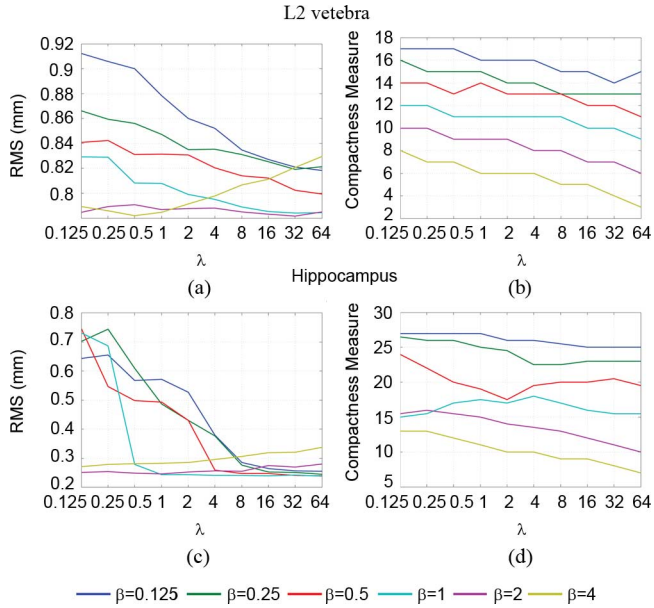

Fig. 1. (a), (c) Generalization and (b), (d) compactness of the model built using different values of parameters, γ and β. (a) Generalization. (b) Compactness. (c) Generalization. (d) Compactness.

B. Comparison to Other Methods

1) L2 Vertebrae: We generated the SSM of L2 vertebrae using the proposed group-wise GMM-based registration and performing PCA as explained earlier. Training point sets are resampled to include 2000 points. The SSM is reconstructed with 1500 points. We found this number of point sufficient to represent the main structures of the vertebra. Parameters of the registration were set to be $\gamma = 16$ and $\beta = 1.0$. This value of γ and β gives the best compromise between generalization and compactness. Fig. 2(a) illustrates the changes in the shape of the vertebra SSM which is reconstructed using the proposed method. The first mode of the shape variation is mainly a scaling in size of the vertebra whereas the second and the third modes involve an expansion of the vertebra body in the lateral direction and changes over length and rotation of the transverse processes. The amount of the variation is color coded for each mode.

Fig. 3(a)–(d) shows the comparison of different methods in terms of generalization G(c), specificity S(c), and compactness C(c), as a function of the number of shape parameters, c, used in the reconstruction [37]. The best SSM should have the lowest generalization, lowest specificity, and highest compactness for the same number of modes. Since the SPHARM-PDM is limited to closed surfaces, we filled the vertebrae hole. The SSM which is built using SPHARM-PDM statistically has the significant lowest Hausdorff distance. However, the model give the worst results in terms of specificity. Excluding the SPHARM-PDM result, the EM-ICP has the worst generalization but the best specificity and compactness, meaning that it generally generates valid instances using few parameters, however, it cannot generate all possible variations. Congealing and group-wise GMM show almost the same behavior except that the group-wise GMM is more compact. The SSM built using the method proposed by Chui and Rangarajan has better compactness and specificity than the group-wise GMM-based technique but worse generalization.

Fig. 4(a)–(e) shows the distance error, overlaid on the mean shape. Except SPHARM-PDM where errors are propagated irregularly, higher errors are mainly observed in extremities parts such as transverse processes and spinous process.

2) Hippocampi Data: Fig. 2(b) illustrates the changes in the shape of the hippocampi models that result from changing the weights corresponding to the first four modes of the variation. The first mode represents mainly scaling whereas the other three represent the stretching of different parts of this anatomy. Similar to the previous section, the SSM built using the proposed method and the other methods are compared in Fig. 3(e)–(h).

EM-ICP behaves the same on hippocampi as in the case of the L2 vertebra. It has the best specificity and compactness but the worst generalization. Also, it has the largest rms distance error. SPHARM-PDM shows better results on this data set. It has the best generalization together with the group-wise GMM-based technique but the worst specificity, meaning that its instances

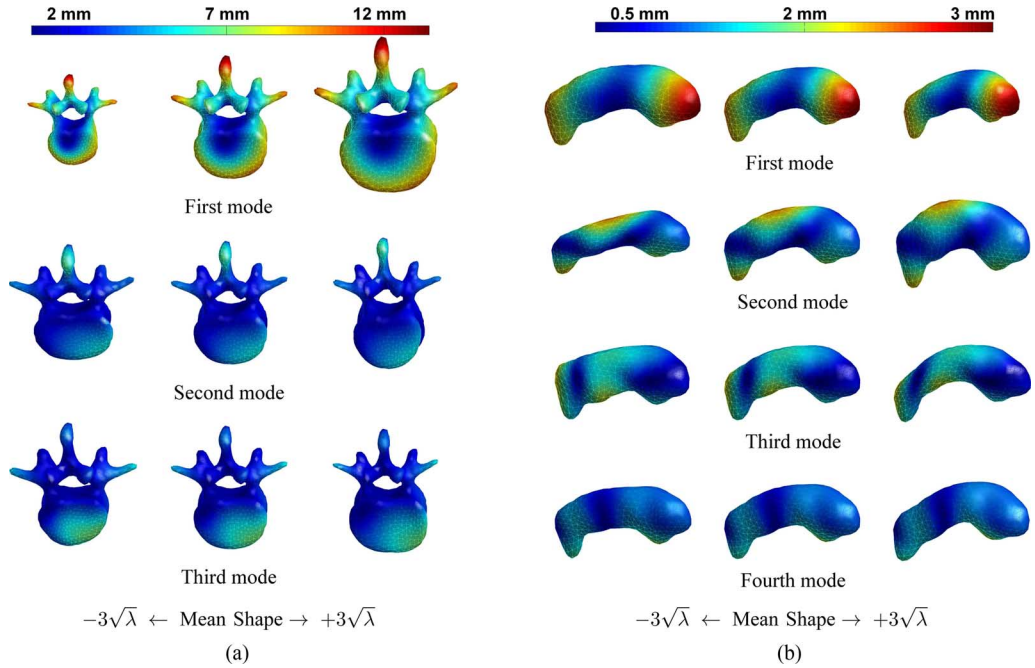

Fig. 2. Graphical representation of the (a) L2 vertebrae and (b) hippocampi shapes described by the SSM after varying the weights corresponding to the first three and four principal modes of variation by 3σ. The amount of variation is color coded for each mode. Higher variations are shown in red. The vertebrae are viewed from superior, and the hippocampi are viewed from inferior.

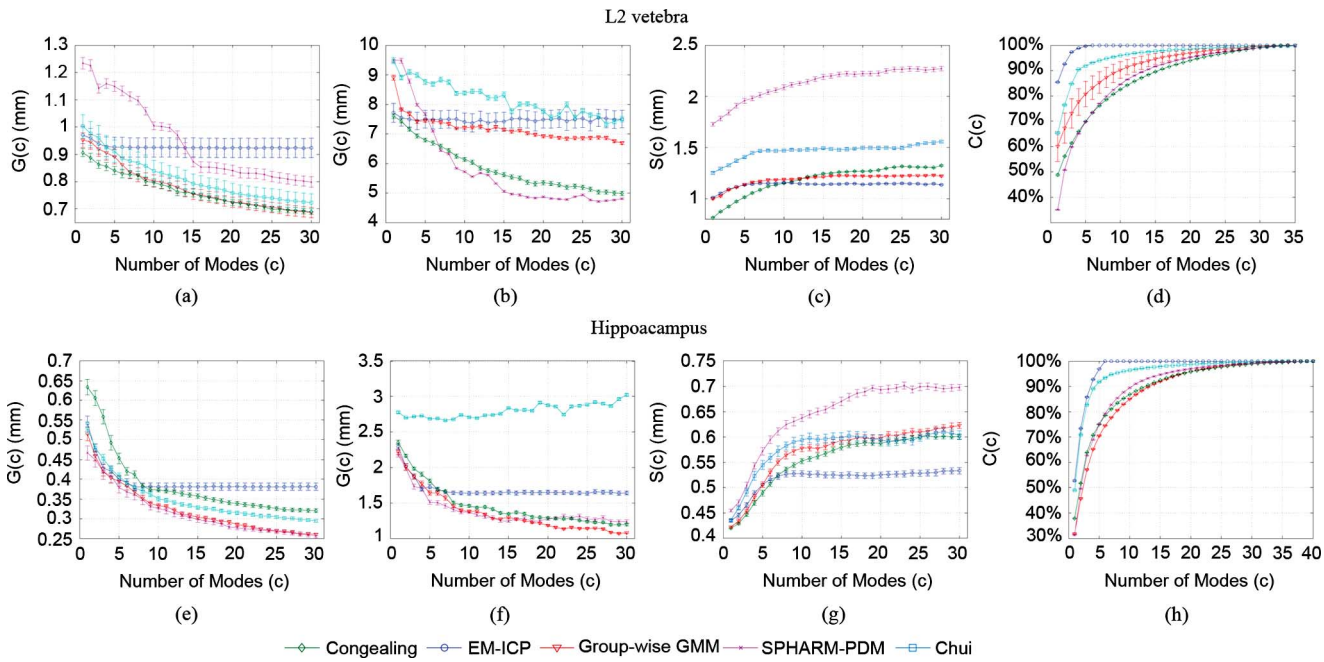

Fig. 3. Generalization, specificity, and compactness ability of the L2 vertebra and hippocampus shape models. Error bars show the standard deviation divided by square root of the number of trials. (a) Generalization (rms). (b) Generalization (Haussdorf). (c) Specificity. (d) Compactness. (e) Generalization (rms). (f) Generalization (Haussdorf). (g) Specificity (h) Compactness.

are likely to be nonrealistic. Congealing has the worst generalization with rms distance error using small number of modes (i.e., $c < 8$), but it shows better results than EM-ICP using more number of modes. It also has substantially worse generalization than group-wise GMM and SPHARM-PDM. Chui's method result in a SSM with better compactness and specificity than the group-wise GMM-based but worse generalization. Fig. 4(g)–(k) shows the distance error, overlaid on the mean shape. Despite L2 vertebra, errors are propagated irregularly on the hippocampi dataset.

C. GMM-ASM Algorithm

An example of a registration of the SSM to a target using proposed GMM-ASM algorithm is shown in Fig. 5. Fig. 6 shows the result of the registration in the presence of noise and outliers using different approaches. Quantitative results are shown

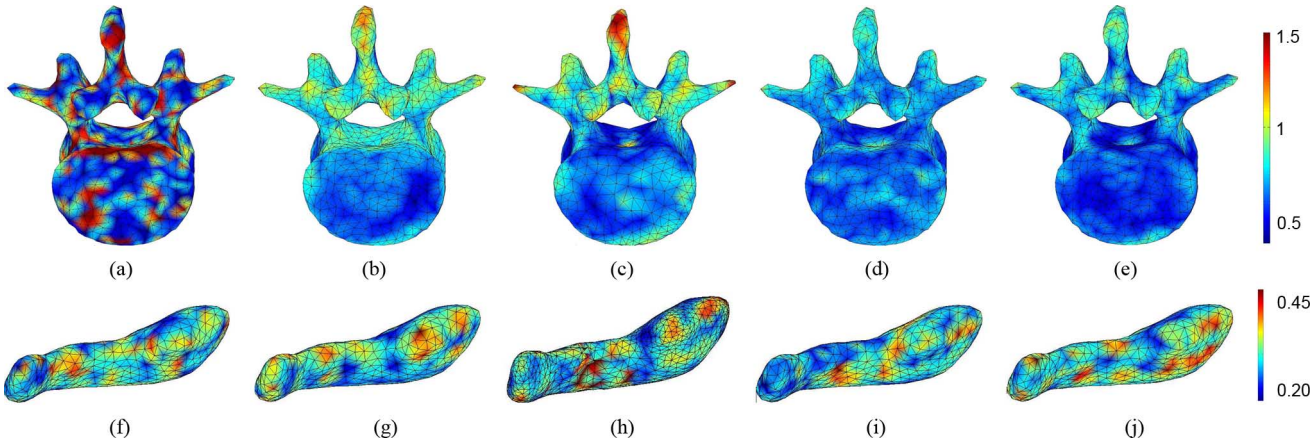

Fig. 4. Distance error is overlaid on the surface of the mean shape built using different approaches. Higher distance is shown in red. For better visualization, hippocampi are viewed from medial, and distances higher than 1.5 mm in vertebra SSM and higher than 0.5 mm in hippocampus SSM are shown in the same color. (a) SPHARM-PDM. (b) EM-ICP. (c) Chui. (d) Congealing. (e) Group-wise GMM. (f) SPHARM-PDM. (g) EM-ICP. (h) Chui. (i) Congealing. (j) Group-wise GMM.

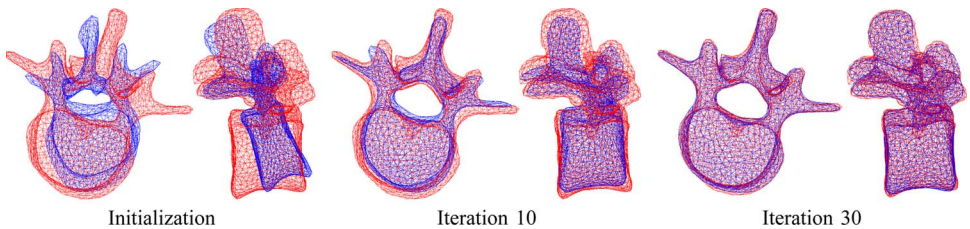

Fig. 5. Example of SSM (shown in blue) to a target (shown in red) registration using GMM-ASM.

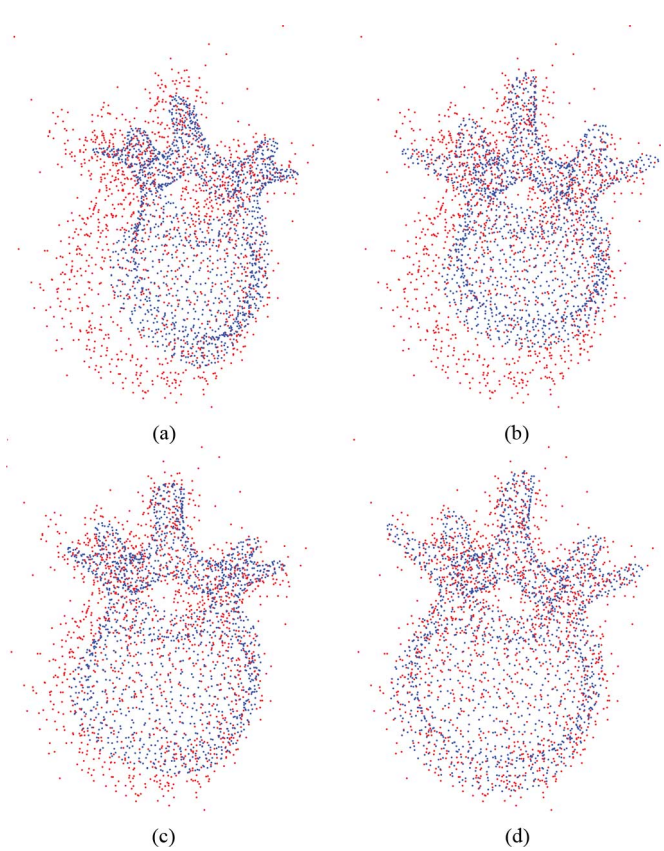

Fig. 6. Registration scenario with 10% outliers and Gaussian additive noise with 3 mm standard deviation. Registration results are presented for (a) the original ASM implementation, (b) WLS-ASM, (c) LMedS-ASM, and (d) our proposed algorithm, GMM-ASM. Blue points are the model whereas red points are the target (a) Original ASM, (b) WLS-ASM, (c) LMedS-ASM, and (d) GMM-ASM.

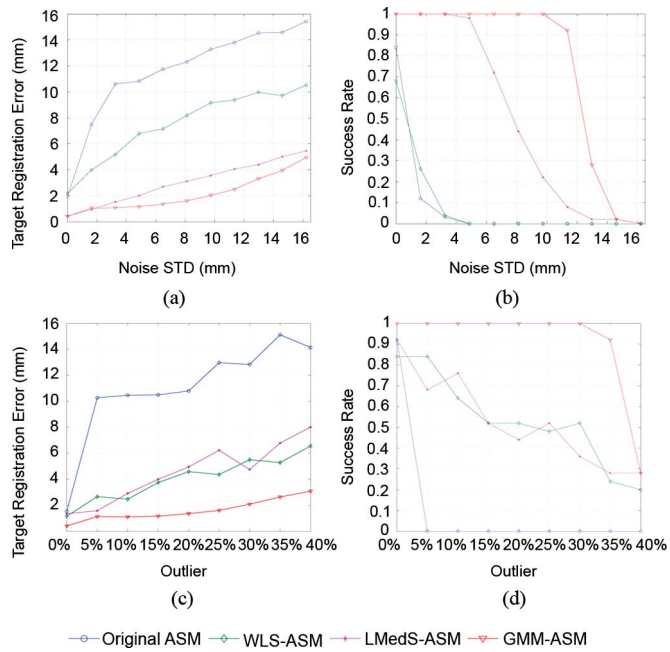

Fig. 7. Robustness of the algorithm against additive noise (a) and (b) and outliers (c) and (d). (a) TRE against additive noise. (b) Success rate against additive noise. (c) TRE against outliers. (d) Success rate against outliers.

in Fig. 7. The original ASM approach most likely converges to a local minimum. It is highly sensitive to the amount of additive noise and outliers. The results are improved using both WLS-ASM and LMedS-ASM. The proposed method is, however, substantially less sensitive to both outliers and additive noise. The success rate remains above 90% with 35% of outliers or additive noise with 10 mm standard deviation.

V. Discussion

The common steps in all group-wise registration techniques is the registration of the mean shape to the instances. Establishing correct correspondences and subsequently identifying the variations are strongly dependent on the accuracy of such registration. However, a registration with perfect alignment but no regularization over the transformation may create incorrect correspondences since the exact anatomical correspondence may not exist. The best tradeoff is usually achieved by changing the regularization factor used in the registration. As shown in Fig. 1(a)–(c), very large and small values of regularization parameters, γ and β, lead to low generalization ability.

We compared our technique to four state-of-the-art group-wise registration techniques using two datasets, L2 lumbar vertebra ($K = 45$) and hippocampi ($K = 42$). The most similar method to ours is the EM-ICP method [23], which utilizes the affine transformation to establish the transformation between the mean shape and the instances. Although the SSM built using this technique is the most compact model [see Fig. 3(d) and (h)], the affine transformation may lead to a large residual between the registered mean shape and the instances. Consequently, the model is not capable of generating all possible variations and predicting an unseen observation [see Fig. 3(a) and (e)]. On the other hand, the limited number of variations prohibits the model from generating invalid variations [see better specificity of the model built using EM-ICP among other models in Fig. 3(c) and (g)].

Our technique is also similar to the one proposed by Chui and Rangarajan [14]. They use a backward model to align all shapes to a reference coordinate and update the mean shape iteratively. That approach is computationally intensive, since it requires reparameterization of the shapes in each iteration. On the other hand, our technique uses a forward model, which is less computationally demanding. Our MATLAB implementation of the algorithm proposed by Chui and Rangarajan takes more than 18 h whereas the MATLAB implementation of group-wise GMM takes less than 1 h. The result demonstrates that our technique generates SSM with better generalization and specificity but worse compactness.

The model built using the SPHARM-PDM method, shows the best generalization and acceptable compactness among other techniques in the hippocampi data, but the worst specificity in both L2 vertebra and hippocompi datasets. The SPHARM-PDM is limited to closed surfaces. To overcome this limitation, we filled the vertebrae hole. But the resulting model still does not provide the best compromise between different measures. The distance errors overlaid on the vertebra mean shape reveal that the higher errors are mainly observed in facet joints, transverse processes and spinous process of the vertebra. In the hippocampi data, higher errors are distributed irregularly. We ran all the other algorithm with the parameters suggested by the original authors [23], [36].

We also compared our proposed technique of registering the SSM to a new observation, GMM-ASM, to the conventional ASM approach. We showed that GMM-ASM algorithm is less sensitive to outliers and additive noise.

VI. Conclusion

We presented a new method to register group of point sets. We utilized the forward modelling and sought for a mean shape and its transformations to each given point set. We formulated the problem as an estimation of the probabilistic density function and used the EM algorithm to solve it. We used the resulted mean shape and transformations to generate a statistical shape model. We also developed a probabilistic method to register the model to a new observation. We performed experiments on two data sets and showed that the overall performance of the proposed algorithm is better than the state-of-the-art techniques.

References

[1] J. Abi-Nahed, M. Jolly, and G. Yang, "Robust active shape models: A robust, generic and simple automatic segmentation tool," *Med. Image Comput. Comput.-Assist. Intervention—MICCAI*, vol. 4191, pp. 1–8, 2006.

[2] N. Amenta, M. Bern, and M. Kamvysselis, "A new Voronoi-based surface reconstruction algorithm," in *Proc. 25th Annu. Conf. Comput. Graphics Interactive Tech.*, 1998, pp. 415–421.

[3] B. Avants and J. C. Gee, "Geodesic estimation for large deformation anatomical shape averaging and interpolation," *NeuroImage*, vol. 23, pp. S139–S150, 2004.

[4] S. K. Balci, P. Golland, M. Shenton, and W. M. Wells, "Free-form B-spline deformation model for groupwise registration," *Med. Image Comput. Comput.-Assist. Intervent.—MICCAI*, vol. 10, pp. 23–30, 2007.

[5] S. K. Balci, P. Golland, and W. Wells, "Non-rigid groupwise registration using b-spline deformation model," *Open Source and Open Data for MICCAI*, pp. 105–121, 2007.

[6] D. C. Barrat, C. S. K. Chan, P. J. Edwards, G. P. Penney, M. Slomczykowski, T. J. Carter, and D. J. Hawkes, "Instantiation and registration of statistical shape models of the femur and pelvis using 3D ultrasound imaging," *Med. Image Anal.*, vol. 12, no. 3, pp. 358–374, 2008.

[7] P. J. Besl and N. D. McKay, "A method for registration of 3-D shapes," *IEEE Trans. Pattern Anal. Mach. Intell.*, vol. 14, no. 2, pp. 239–256, Feb. 1992.

[8] K. K. Bhatia, J. V. Hajnal, B. K. Puri, A. D. Edwards, and D. Rueckert, "Consistent groupwise non-rigid registration for atlas construction," in *Proc. IEEE Int. Symp. Biomed. Imag.: Nano to Macro*, 2004, vol. 1, pp. 908–911.

[9] C. M. Bishop, *Pattern Recognition and Machine Learning*. New York: Springer, 2006.

[10] F. L. Bookstein, "Landmark methods for forms without landmarks: morphometrics of group differences in outline shape," *Med. Image Anal.*, vol. 1, no. 3, pp. 225–243, 1997.

[11] A. D. Brett and C. J. Taylor, "A method of automated landmark generation for automated 3D PDM construction," *Image Vis. Comput.*, vol. 18, no. 9, pp. 739–748, 1999.

[12] T. Chen, B. C. Vemuri, A. Rangarajan, and S. J. Eisenschenk, "Group-wise point-set registration using a novel CDF-based Havrda-Charvtat divergence," *Int. J. Comput. Vis.*, vol. 86, no. 1, pp. 111–124, 2010.

[13] H. Chui and A. Rangarajan, "A new point matching algorithm for non-rigid registration," *Comput. Vis. Image Understand.*, vol. 89, no. 2–3, pp. 114–141, 2003.

[14] H. Chui, A. Rangarajan, J. Zhang, and C. M. Leonard, "Unsupervised learning of an atlas from unlabeled point-sets," *IEEE Trans. Pattern Anal. Mach. Intell.*, vol. 26, no. 2, pp. 160–172, Feb. 2004.

[15] T. F. Cootes, A. Hill, C. J. Taylor, and J. Haslam, "Use of active shape models for locating structures in medical images," *Image Vis. Comput.*, vol. 12, no. 6, pp. 355–365, 1994.

[16] T. F. Cootes, C. J. Taylor, D. H. Cooper, and J. Graham, "Active shape models-their training and application," *Comput. Vis. Image Understand.*, vol. 61, no. 1, pp. 38–59, 1995.

[17] T. F. Cootes, C. J. Twining, K. O. Babalola, and C. J. Taylor, "Diffeomorphic statistical shape models," *Image Vis. Comput.*, vol. 26, no. 3, pp. 326–332, 2008.

[18] R. H. Davies, C. J. Twining, T. F. Cootes, J. C. Waterton, and C. J. Taylor, "A minimum description length approach to statistical shape modeling," *IEEE Trans. Med. Imag.*, vol. 21, no. 5, pp. 525–537, May 2002.

[19] I. Dryden and K. V. Mardia, *The Statistical Analysis of Shape*. New York: Wiley, 1998.

[20] S. Durrleman, X. Pennec, A. Trouvte, and N. Ayache, "Statistical models of sets of curves and surfaces based on currents," *Med. Imag. Anal.*, vol. 13, no. 5, pp. 793–808, 2009.

[21] M. A. Fischler and R. C. Bolles, "Random sample consensus: a paradigm for model fitting with applications to image analysis and automated cartography," *Commun. ACM*, vol. 24, no. 6, pp. 381–395, 1981.

[22] T. Heimann and H. P. Meinzer, "Statistical shape models for 3d medical image segmentation: A review," *Med. Imag. Anal.*, vol. 13, no. 4, pp. 543–563, 2009.

[23] H. Hufnagel, X. Pennec, J. Ehrhardt, N. Ayache, and H. Handels, "Generation of a statistical shape model with probabilistic point correspondences and the expectation maximization-iterative closest point algorithm," *Int. J. Comput. Assist. Radiol. Surg.*, vol. 2, no. 5, pp. 265–273, 2008.

[24] S. Joshi, B. Davis, M. Jomier, and G. Gerig, "Unbiased diffeomorphic atlas construction for computational anatomy," *NeuroImage*, vol. 23, pp. S151–S160, 2004.

[25] H. Li and O. Chutatape, "Automated feature extraction in color retinal images by a model based approach," *IEEE Trans. Biomed. Eng.*, vol. 51, no. 2, pp. 246–254, Feb. 2004.

[26] C. Lorenz and N. Krahnstover, "Generation of point-based 3D statistical shape models for anatomical objects," *Comput. Vis. Image Understand.*, vol. 77, no. 2, pp. 175–191, 2000.

[27] G. J. McLachlan and D. Peel, *Finite Mixture Models*. New York: Wiley-Interscience, 2000.

[28] S. Milborrow and F. Nicolls, "Locating facial features with an extended active shape model," *Comput. Vis. ECCV 2008*, vol. 5305, pp. 504–513, 2008.

[29] A. Myronenko and X. Song, "Point set registration: coherent point drift," *IEEE Trans. Pattern Anal. Mach. Intell.*, vol. 32, no. 12, pp. 2262–2275, Dec. 2010.

[30] A. Myronenko, X. Song, and M. Carreira-Perpinan, "Non-rigid point set registration: Coherent point drift," in *Advances in Neural Information Processing Systems (NIPS)*. Cambridge, MA: Cambridge, 2007, vol. 19, pp. 1009–1016.

[31] S. M. Pizer, P. T. Fletcher, S. Joshi, A. Thall, J. Z. Chen, Y. Fridman, D. S. Fritsch, A. G. Gash, J. M. Glotzer, M. R. Jiroutek, C. Lu, K. E. Muller, G. Tracton, P. Yushkevich, and E. L. Chaney, "Deformable m-reps for 3D medical image segmentation," *Int. J. Comput. Vis.*, vol. 55, no. 2, pp. 85–106, 2003.

[32] M. Rogers and J. Graham, "Robust active shape model search," *Comput. Vis. ECCV 2002*, vol. 2353, pp. 289–312, 2006.

[33] P. J. Rousseeuw, *Robust Regression and Outlier Detection*. New York: Wiley, 1987.

[34] D. Rueckert, A. F. Frangi, and J. A. Schnabel, "Automatic construction of 3D statistical deformation models of the brain using nonrigid registration," *IEEE Trans. Med. Imag.*, vol. 22, no. 8, pp. 1014–1025, Aug. 2003.

[35] K. Seshadri and M. Savvides, "Robust modified active shape model for automatic facial landmark annotation of frontal faces," in *Proc. IEEE 3rd Int. Conf. Biometrics: Theory, Appl., Systems*, 2009, pp. 1–8.

[36] M. Styner, I. Oguz, S. Xu, C. Brechbuhler, D. Pantazis, J. J. Levitt, M. E. Shenton, and G. Gerig, "Framework for the statistical shape analysis of brain structures using SPHARM-PDM," *Insight J.*, pp. 1–20, 2006.

[37] M. Styner, K. Rajamani, L. Nolte, G. Zsemlye, G. Szekely, C. Taylor, and R. Davies, "Evaluation of 3D correspondence methods for model building," *Inform. Process. Med. Imag.*, vol. 2732, pp. 63–75, 2003.

[38] C. J. Twining, T. Cootes, S. Marsland, V. Petrovic, R. Schestowitz, and C. J. Taylor, "A unified information-theoretic approach to groupwise non-rigid registration and model building," *Inform. Process. Med. Imag.*, vol. 3565, pp. 1–14, 2005.

[39] F. Wang, B. C. Vemuri, and A. Rangarajan, "Groupwise point pattern registration using a novel CDF-based Jensen-Shannon divergence," in *Proc. IEEE Comput. Soc. Conf. Comput. Vis. Pattern Recognit.*, 2006, vol. 1, pp. 1283–1288.

[40] Q. Wang, L. Chen, P. Yap, G. Wu, and D. Shen, "Groupwise registration based on hierarchical image clustering and atlas synthesis," *Human Brain Map.*, vol. 31, no. 8, pp. 1128–1140, 2010.

[41] A. L. Yuille and N. M. Grzywacz, "The motion coherence theory," in *Proc. Int. Conf. Comput. Vis.*, 1998, vol. 3, pp. 344–353.

[42] A. L. Yuille and N. M. Grzywacz, "The motion coherence theory," in *Proc. Int. Conf. Comput. Vis.*, 1988, pp. 344–353.

[43] P. A. Yushkevich, J. Piven, H. C. Hazlett, R. G. Smith, S. Ho, J. C. Gee, and G. Gerig, "User-guided 3D active contour segmentation of anatomical structures: significantly improved efficiency and reliability," *Neuroimage*, vol. 31, no. 3, pp. 1116–1128, 2006.

[44] Z. Zhao and E. K. Teoh, "A novel framework for automated 3 D PDM construction using deformable models," *Proc. SPIE Med. Imag.*, vol. 5747, pp. 303–314, 2005.

[45] P. J. Huber, *Robust Statistics*. New York: Wiley, 1981.

[46] M. Rogers and J. Graham, "Robust active shape model search," in *Computer Vision — ECCV*, 2006, vol. 2353, pp. 289–312.